PROCEEDINGS OF SPIE

Electromagnetic characterization of white spruce at different moisture contents using synthetic aperture radar imaging

Christopher M. Ingemi, Jones Owusu Twumasi , Tzuyang Yu

SPIE.

Electromagnetic Characterization of White Spruce at Different Moisture Contents using Synthetic Aperture Radar Imaging

Christopher M. Ingemi, Jones Owusu Twumasi, Tzuyang Yu

Department of Civil and Environmental Engineering

University of Massachusetts Lowell

One University Avenue, Lowell, MA 01854, U.S.A.

ABSTRACT

Detection and quantification of moisture content inside wood (timber) is key to ensuring safety and reliability of timber structures. Moisture inside wood attracts insects and fosters the development of fungi to attack the timber, causing significant damages and reducing the load bearing capacity during their design life. The use of non-destructive evaluation (NDE) techniques (e.g., microwave/radar, ultrasonic, stress wave, and X-ray) for condition assessment of timber structures is a good choice. NDE techniques provide information about the level of deterioration and material properties of timber structures without obstructing their functionality. In this study, microwave/radar NDE technique was selected for the characterization of wood at different moisture contents. A 12 in-by-3.5 in-by-1.5 in. white spruce specimen (picea glauca) was imaged at different moisture contents using a 10 GHz synthetic aperture radar (SAR) sensor inside an anechoic chamber. The presence of moisture was found to increase the SAR image amplitude as expected. Additionally, integrated SAR amplitude was found beneficial in modeling the moisture content inside the wood specimen.

Keywords: Microwave/radar NDE, wood, moisture content, synthetic aperture radar

1. INTRODUCTION

For many generations, wood (timber) has been one of the most widely used construction materials throughout the world. The availability of wood as a renewable resource, its ease of assembly, and its affordable price all contribute to making it a remarkable building material for small to mid-rise construction projects.[1] The majority of single family residences in the United States are constructed from dimension lumber. Of the $1.2 trillion dollars spent annually on construction in the U.S., 51% of that money is spent on the construction of single family homes.[2] White Spruce (picea glauca), which grows within USDA hardiness zones 2-6, covering most of the US and Canada, is one of the most frequently used building material in North America.[3]

An increasing focus on sustainable construction practices, in recent years, makes it highly important to get the maximum service life out of an existing structure. With proper preventative maintenance, periodic inspection, and protection from the elements, timber structures can last for centuries, reducing the consumption of construction materials. One of the biggest contributors to the premature failure of wood structures is the presence of moisture. The moisture contained in wood is held in two ways. The moisture within the cell cavity of a wood specimen is referred to as free water and is the first to be released as the wood dries. Bound water is the moisture held within the cell walls and is not released until all of the free water is driven off. The point when all of the free water has been released and all of the bound water remains is referred to as the fiber saturation point (FSP). For most species FSP is about 30% moisture content.[1] Tests performed by The U.S. Forest Service and the U.S. Forest Products Laboratory have found that the modulus of rupture in static bending, the fiber stress at the elastic limit in static bending, the fiber stress at the elastic limit in compression parallel to the grain, and the maximum crushing stress in compression parallel to the grain all increase as moisture content (MC) decreases below the FSP.[4] In addition to loss of strength at higher MC, the presence of moisture also causes the

---

Further author information: (Send correspondence to T. Yu)

E-mail: Tzuyang_Yu@uml.edu, Telephone: 1 978 934 2288

wood to become susceptible to further degradation caused by insects such as carpenter ants and termites and fungi such as brown rot fungus.[5]

Evaluation of construction materials using electromagnetic (EM) methods has proven to be useful because of its ability to provide subsurface information. Condition assessment and dielectric modeling of wood materials using EM methods (e.g., microwave/radar) has been previously demonstrated in literature. Reci et. al. evaluated spruce samples at different moisture contents using ground-penetrating radar (GPR) at a frequency of 1.5 GHz.[6] In Sahin et. al., dielectric models of various hardwoods were created at different moisture contents ranging from 0% to 28% based on the Von Hippel transmission line method at microwave frequencies of 9.8 GHz and 2.45 GHz.[7] Synthetic Aperture Radar (SAR) has emerged in recent years as a novel technology for subsurface evaluation because of its remote viewing abilities. While other EM methods such as GPR require contact or near contact inspection conditions, SAR has been shown to have the ability to perform inspection with a range of up to 15 m allowing for considerable freedom when taking measurements.[8]

In this paper, changing moisture contents of a white spruce specimen were evaluated using SAR images at different ranges. The experiment was conducted using a continuous wave imaging radar (CWIR) at 10 GHz. The experimental methods used are provided in this paper. The results and data are analyzed, and finally a summary of the results is presented in the conclusion.

2. SYNTHETIC APERTURE RADAR IMAGING

2.1 Signal Processing
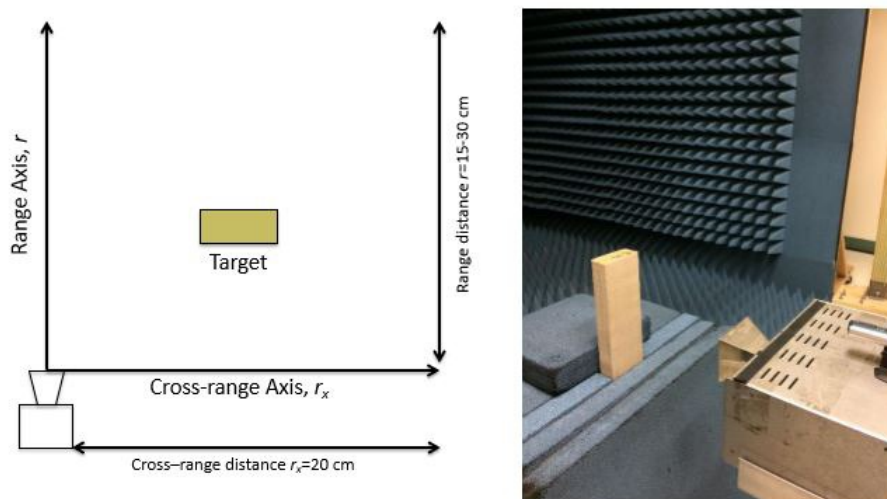
Figure 1. Schematic of stripmap SAR imaging (left), and experimental configuration of SAR imaging inside an anechoic chamber (right)

In stripmap SAR imaging mode strips of surface and subsurface data are collected outward from the radar antenna in the range direction as the radar travels along it's synthetic aperture, perpindicular to the radar in the cross-range direction. Fig.1 shows the SAR imaging configuration used in this experiment. To generate SAR images in the range-cross range domain, backprojection algorithms are used. The backprojected SAR image, I is obtained by:

$$I(\overline{r}, \phi) = \int_0^{\overline{r}_s \theta_{int}} d\varepsilon \cdot B_{BP}(\varepsilon, \hat{t}) \tag{1}$$

where $(\bar{r}, \phi)$ = polar coordinates on the SAR image range cross-range plane, θ_{int} = the synthetic aperture and $B_{BP}(\epsilon, t)$ = the band pass transfer function. More information on the theory behind this process can be found in Yu et. al.[8]

3. EXPERIMENTAL PROCEDURE

3.1 Specimen Preparation

To reduce the effects of changing geometries and surface texture on resulting SAR images, a single specimen was used for all the measurements. A 2x4 (3.5 in. by 1.5 in.) length of white spruce was purchased from a local lumber yard and cut to a length of 12 in. long. The specimen was submerged into a bath of water, and the mass was measured daily as the specimen absorbed the water until the change in mass had stabilized. The moisture content (MC) of the specimen is defined as

$$MC = \frac{M_{actual} - M_{dry}}{M_{dry}} * 100\% \qquad (2)$$

where MC(%) is the percentage of moisture contained in the specimen, M_{actual} is the current mass of the specimen (g), and M_{dry} is the oven dry mass of the specimen (g). After two weeks when the specimen had reached its maximum moisture content, it was removed from the water and the surface moisture was removed with a paper towel. The first SAR measurement was taken after the first hour of being removed from the water bath. SAR Measurements were then taken regularly over a period of two weeks as the specimen air dried. As the MC of the specimen stabilized with the environment it became necessary to further dry the specimen in an oven at 50° C for 12 hours intervals to continue to make SAR measurements. Finally to get the oven dry mass the specimen was put into an oven at 100° C for 24 hours before taking a final SAR measurement. SAR measurements were taken at $MC = 45.1\%, 40.5\%, 35.8\%, 27.8\%, 21.6\%, 16.0\%, 13.3\%, 10.3\%, 9.5\%$ and at oven dried condition $MC = 0.0\%$.

3.2 SAR Image Collection

For this experiment all the radar images were taken inside an anechoic chamber. The specimen was positioned vertically with respect to the radar configuration by taking multiple distance measurements to the wood sample, as shown in Fig.2. A constant cross-range of 20 cm was used for all measurements with the specimen placed at the center. A cross-range step interval of 0.3125 cm was used resulting in 64 scans for each measurement. For comparison 4 different range distances were chosen 15 cm, 20 cm, 25 cm, and 30 cm and were used for every MC evaluated. For each measurement the same surface of the specimen was evaluated in order to reduce the number of variables present.

4. RESULTS AND ANALYSIS

4.1 SAR Images

Shown in Fig.3 are a series of SAR images for different ranges and MC, plotted in the range vs. cross-range domain. Three different MC are displayed in Fig.3 as a representation of the entire spectrum of MC measured in this experiment. In total, there were forty SAR images; one image for every MC at each range. The color scale is used to indicate the magnitude of the SAR amplitudes at given points within the plot. It was evident from observation that as MC of the specimen decreases the amplitude distribution decreases. The maximum amplitudes of the images also decreases with decreasing moisture content. Fig.3 shows plots of amplitude vs. range at the point of maximum amplitude I_{max}, the graph on the left further illustrates the reduction of I_{max} with decreasing MC for r=15 cm. This phenomenon was due to the changing dielectric constant of the material. Wood fiber on its own has a very low dielectric constant, but when the amount of water present in the specimen increases (water having a higher dielectric constant than wood fiber) the dielectric constant of the specimen increases. The material's dielectric constant has a direct effect on the specular returns received by the imaging radars antenna, causing an attenuation of radar signals as the materials dielectric constant decreases. The effect of range on the SAR images was evident by noting the position of the amplitude distribution along the horizontal axis, with increasing range there was an increasing shift in amplitude distribution shown in the right side graph of
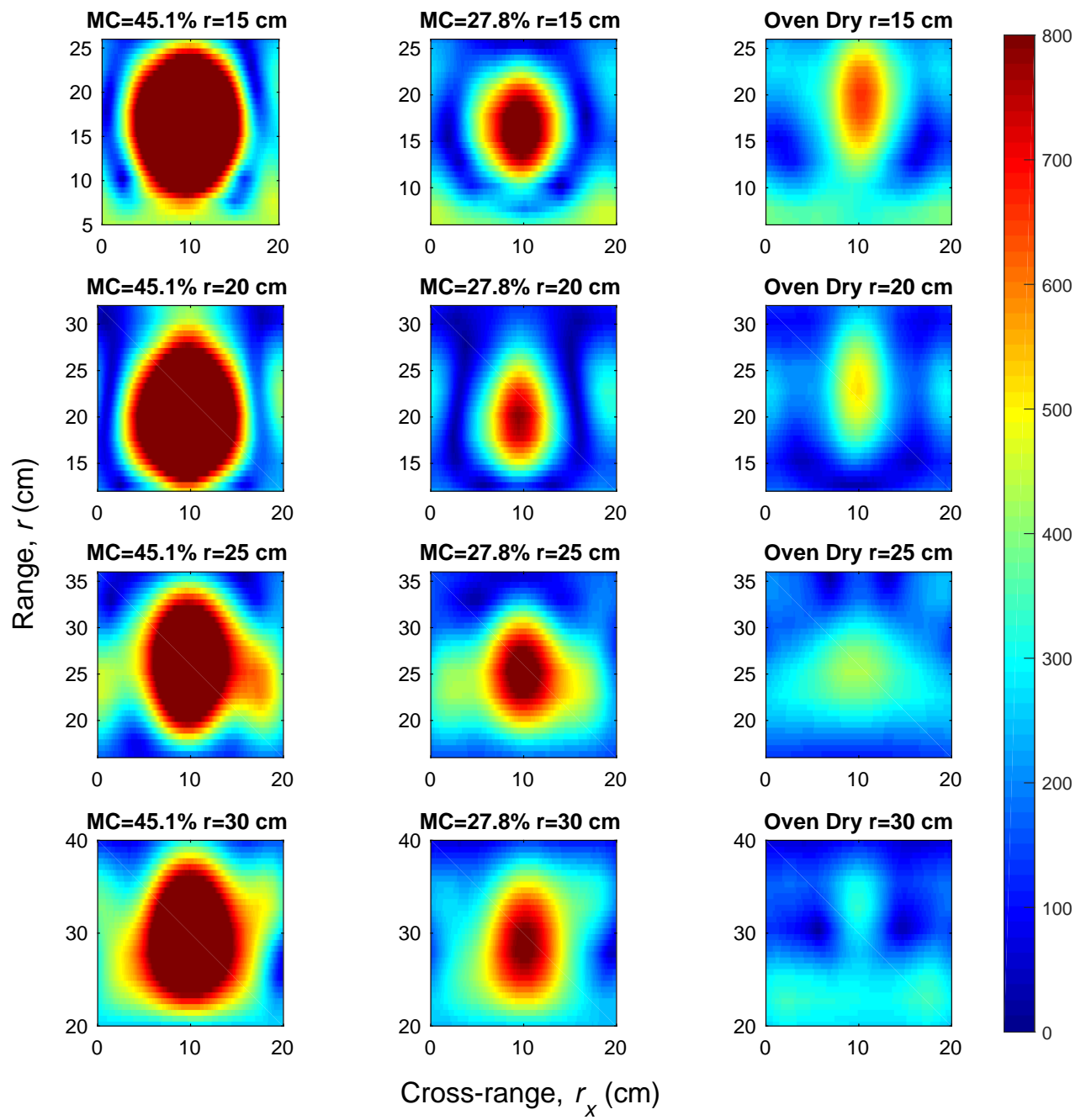
Figure 2. SAR images for r=15 cm, r=20 cm, r= 25 cm, and r= 30 cm at MC=45.1%, MC=27.8%, and MC=Oven Dry
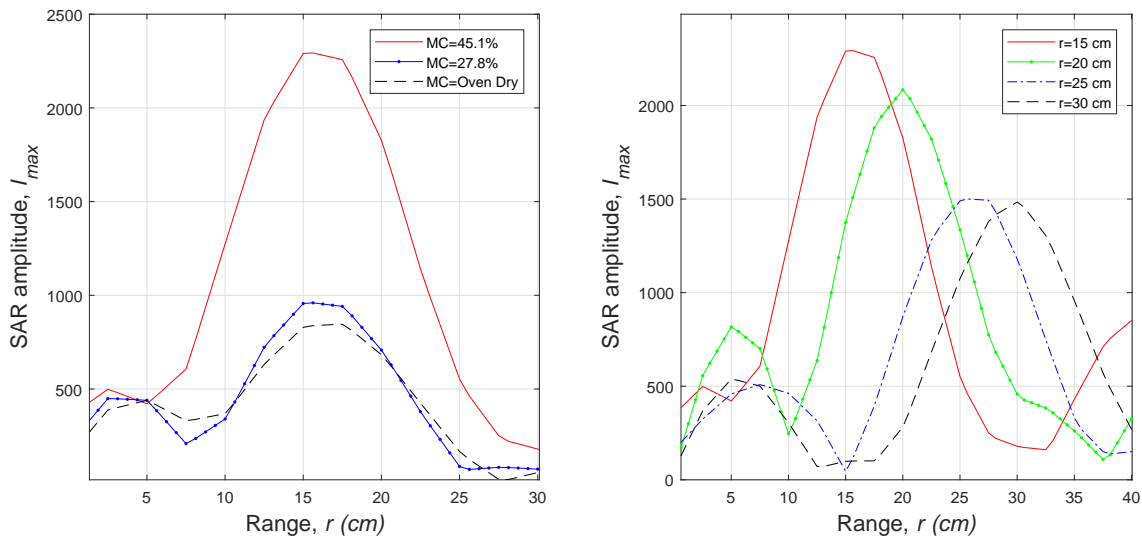
Figure 3. Amplitude vs. range at maximum amplitude for r= 15 cm (left), for range=15 cm, range=20 cm, range=25 cm, and range=30 cm (right)

Fig.3. To some extent there was an attenuation of amplitude distribution as the range increases due to scattering effects. However, because of the material properties and the interaction between the EM waves and dielectric material this does not occur with much consistency.

4.2 Integrated SAR amplitude

The first step in evaluating the amplitude distribution of the SAR images was to sum all of the amplitudes under the curves in Fig.2. Finding the integrated SAR amplitude (I_{SAR}) was a good starting place for analysis because the output is a single value which represents the total specular return reflected off the specimen. Shown in Fig.4 is a plot of I_{SAR} with respect to MC for the four different ranges. As expected I_{SAR} increased with increasing moisture for each of the four ranges investigated. This data was modeled using the second order expotential function in Eq.(3) where $I_{SAR}(\psi)$ = integrated SAR amplitude, C_1, C_2, C_3, and C_4 = constants and ψ = MC.

$$I_{SAR}(\psi) = C_1 \exp[C_2\psi] + C_3 \exp[C_4\psi] \tag{3}$$

In comparison Fig.5 shows these models from all four ranges. The expected results would be that signal

Table 1. Model parameters

Range (cm)	C_1	C_2	C_3	C_4	R^2
15	$9.419 * 10^4$	0.02911	$1.374 * 10^{-10}$	0.7877	0.9483
20	$8.704 * 10^4$	0.01477	4.02	0.2556	0.9585
25	$5.584 * 10^4$	0.03918	$2.629 * 10^{-11}$	0.7944	0.9221
30	$2.482 * 10^5$	0.01450	5.914	0.2243	0.9400
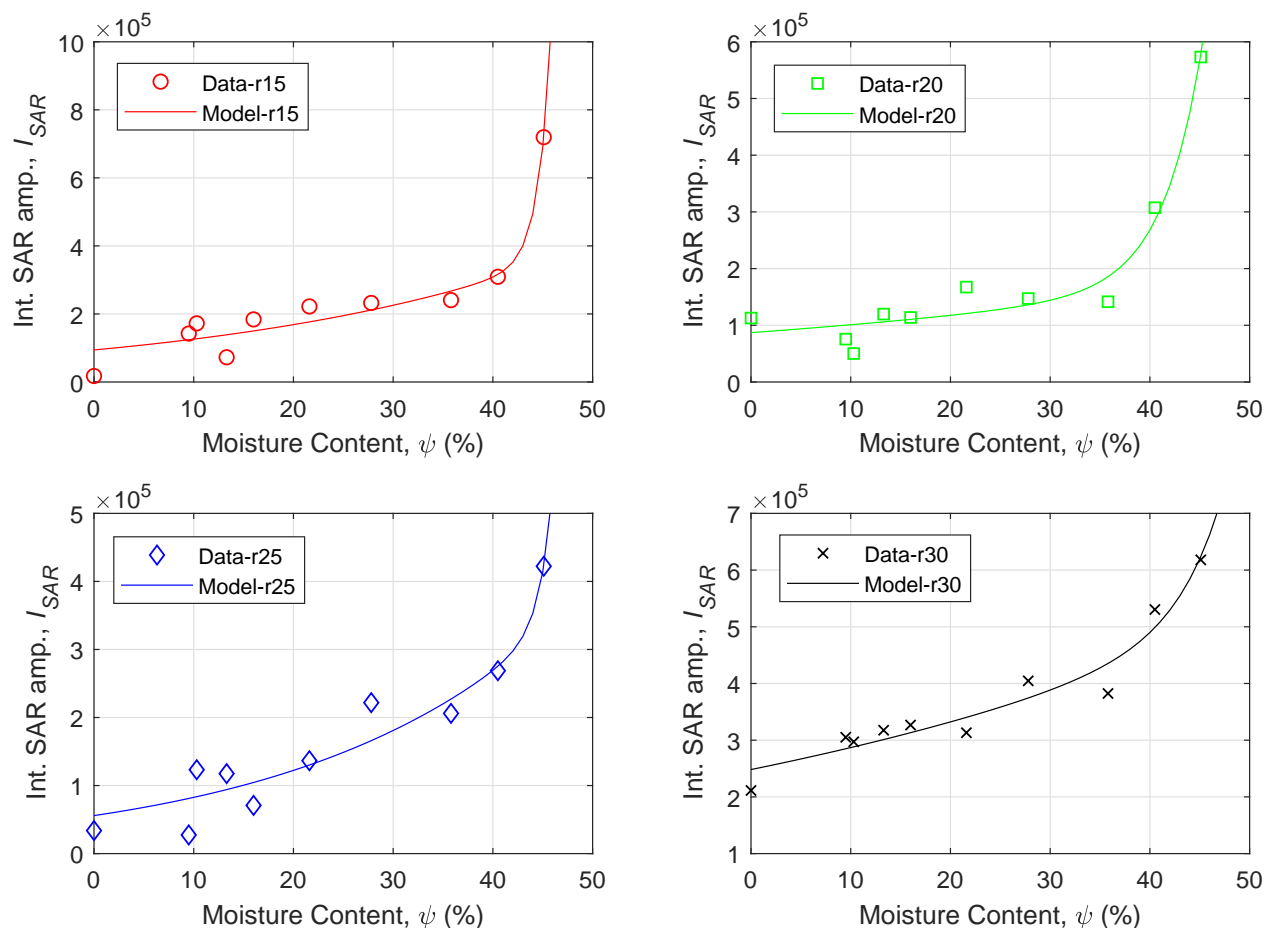
Figure 4. I_{SAR} vs MC for range=15 cm, range=20 cm, range=25 cm, and range=30 cm

attenuation occurs as the range increases due to increasing signal scattering, reducing the corrosponding I_{SAR}, but this does not happen with enough consistency to be able to draw any conclusions. Due to the dielectric nature of the material a complicated interaction was created between the signal and the material at greater ranges causing some unusual responses at r=25 cm and r=30 cm.

4.3 Area contour estimation analysis

A second investigation of the SAR images was conducted by evaluating the area of contour slices taken at various points in the SAR amplitude direction for each moisture content and plotting them with resepect to the amplitude ratio (AR). To begin this process, separately for each of the ranges, the SAR images for all the corrosponding MC are normalized with the maximum amplitude of the image with the largest MC, leaving MC=45.1% to have an amplitude ratio of 1.0. This allows the AR of the images with smaller MC to be represented as a percentage of the maximum amplitude of the largest MC. The AR of each SAR image is then divided equally up into 10 sections. Slices were taken at these ten sections and the areas of the resulting contours were estimated. Naturally the size of these contours will decrease as AR increases. Fig.6 shows for r=30 cm the area of these contours plotted with respect to the AR the slice was taken at. When a linear model was created for every MC it becomes evident that as the moisture content decreases the slope of the linear model increases. This result seems logical because naturally for SAR images with larger AR the change in contour area with respect to amplitude would be very
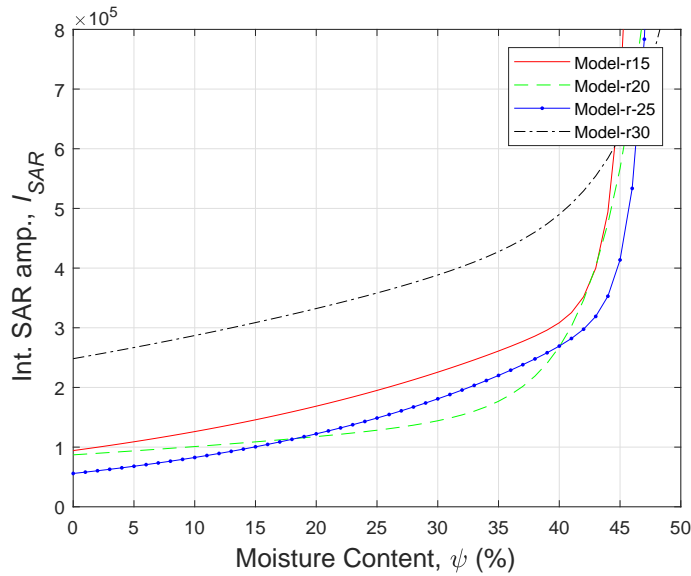
Figure 5. I_{SAR} vs MC for range=15 cm, range=20 cm, range=25 cm, and range=30 cm

gradual when compared to SAR images with smaller AR. Eq.(4) represents this linear model with A=contour area, $\frac{DA}{d\alpha_i}$=slope of the line, α_i=amplitude ratio and C=the y-intercept. Fig.6 only shows the data for range=30 cm but this trend holds true for each of the ranges investigated. To show this relationship in Fig.7 these slopes are plotted with respect to their corrosponding MC. There tends to be a couple of outliers when investigating MC below 16% but the overall trend remains consistant.
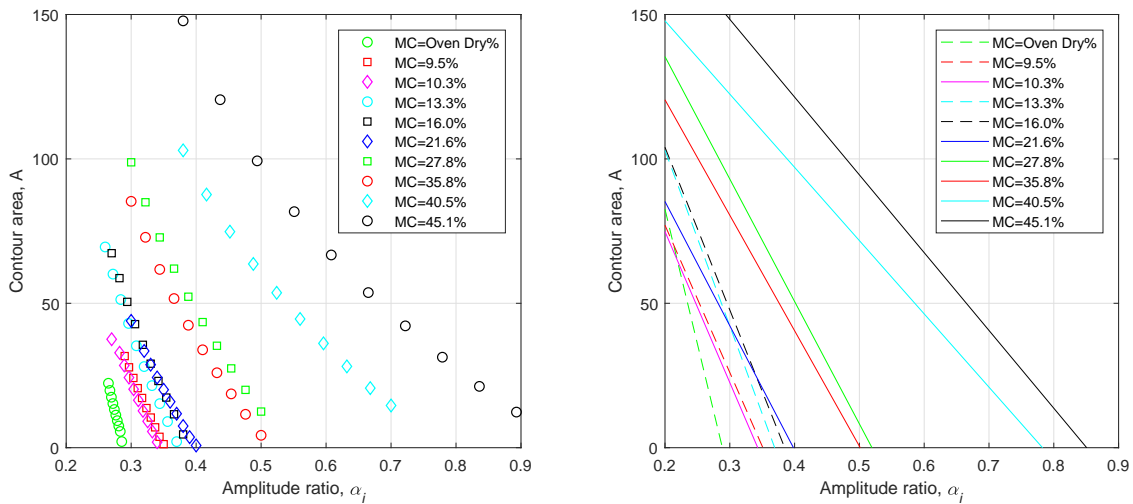
Figure 6. Contour area vs. amplitude for r=30 cm (left), linear models for r=30 cm (right)

$$A = \frac{DA}{d\alpha_i}\alpha_i + C \qquad (4)$$

Table 2. Model parameters

$\psi(\%)$	$\frac{DA}{d\alpha_i}$	C
0.0	-709.8	202.0
9.5	-510.0	179.1
10.3	-522.9	179.4
13.3	-608.3	.224.6
16.0	-563.2	216.7
21.6	-430.1	171.27
27.8	-423.9	220.2
35.8	-399.8	200.4
40.5	-269.3	198.6
45.1	-253.7	229.13

5. CONCLUSION

The use of SAR imaging for evaluating changing moisture contents in a sample of white spruce is explored. It is found that the presence of moisture (because of the high dielectric constant of water) increases the SAR amplitude distribution and the integrated SAR amplitude. It is also found, by calculating the area of countour slices taken in the amplitude direction of the SAR images and plotting them with respect to amplitude ratio, that moisture content can be determined by creating linear models of this data. Range has an effect on the position of the SAR amplitude distribution along the range-axis but could not be determined for observing the size of the amplitude distribution. These positive results confirm that SAR imaging can be a useful tool for the detection moisture in wood structures.

6. ACKNOWLEDGMENT

REFERENCES

1. D. E. Breyer, K. J. Fridley, J. D. G. Pollock, and K. Cobeen, *Design Of Wood Structures-Asd/Lrfd*, McGraw Hill, 2015.
2. D. T. Damery, P. Clouston, and P. R. Fisette, "Wood science education in a changing world a case study of the umass-amherst building materials and wood technology program, 1965-2005," *Forest Products Journal* **57**(5), pp. 19–24, 2007.
3. E. F. Gilman and D. G. Watson, "Picea omorika serbian spruce fact sheet st-450," *Environmental Horticulture Department, Florida Cooperative Extension Service, University of Florida* , 1994.
4. T. R. C. Wilson, *Strength-moisture relations for wood*, no. 282, US Dept. of Agriculture, 1932.
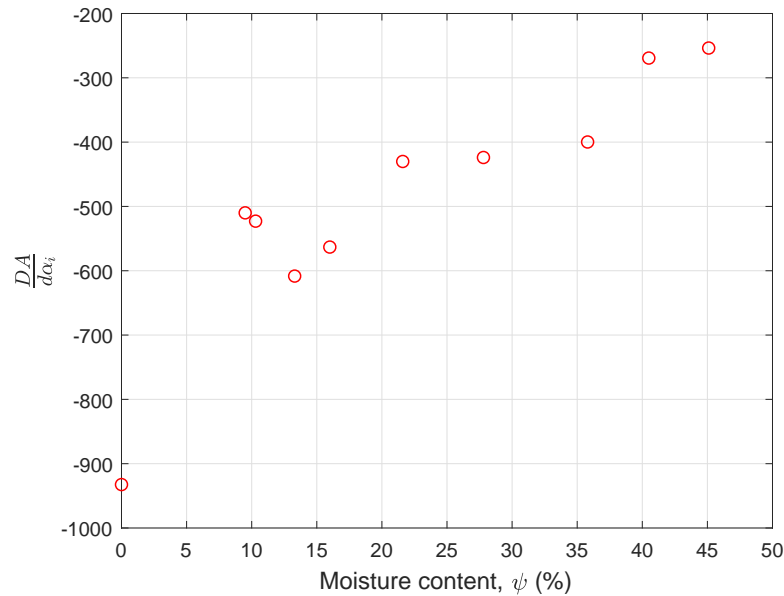
Figure 7. Slope of contour area vs. MC (%) for r=30 cm

5. M. E. Weaver, "Successes and failures in the conservation of wooden structures," *Journal of Architectural Conservation* **9**(3), pp. 36–50, 2003.

6. H. Reci, C. M. Tien, Z. M. Sbartaï, L. Pajewski, and E. Kiri, "Non-destructive evaluation of moisture content in wood using ground-penetrating radar," *Geoscientific Instrumentation, Methods and Data Systems* **5**(2), p. 575, 2016.

7. H. Sahin and N. Ay, "Dielectric properties of hardwood species at microwave frequencies," *Journal of Wood Science* **50**(4), pp. 375–380, 2004.

8. T. Yu, J. O. Twumasi, V. Le, Q. Tang, and N. D'Amico, "Surface and subsurface remote sensing of concrete structures using synthetic aperture radar imaging," *Journal of Structural Engineering* **143**(10), p. 04017143, 2017.